Nonlinear Differ. Equ. Appl. (2017) 24:37

1021-9722/17/040001-25
published online June 15, 2017
DOI 10.1007/s00030-017-0461-y

Nonlinear Differential Equations and Applications NoDEA

On the uniqueness of vanishing viscosity solutions for Riemann problems for polymer flooding

Wen Shen

Abstract. We consider the vanishing viscosity solutions of Riemann problems for polymer flooding models. The models reduce to triangular systems of conservation laws in a suitable Lagrangian coordinate, which connects to scalar conservation laws with discontinuous flux. These systems are parabolic degenerate along certain curves in the domain. A vanishing viscosity solution based on a partially viscous model is given in a parallell paper (Guerra and Shen in Partial Differ Equ Math Phys Stoch Anal: 2017). In this paper the fully viscous model is treated. Through several counter examples we show that, as the ratio of the viscosity parameters varies, infinitely many vanishing viscosity limit solutions can be constructed. Under some further monotonicity assumptions, the uniqueness of vanishing viscosity solutions for Riemann problems can be proved.

Mathematics Subject Classification. Primary 35L65, Secondary 35L80, 35L60.

Keywords. Conservation laws, Riemann problems, Vanishing viscosity, Parabolic degeneracy, Discontinuous flux, Polymer flooding.

1. Introduction

In this paper we study the uniqueness of the solutions of Riemann problems for some systems of conservation laws, obtained as the vanishing viscosity limit. In particular, we consider the equations for polymer flooding in secondary oil recovery

$$\begin{cases} s_t + f(s,c)_x = 0, \\ (m(c) + cs)_t + (cf(s,c))_x = 0. \end{cases} \tag{1.1}$$

This article is part of the topical collection "Hyperbolic PDEs, Fluids, Transport and Applications: Dedicated to Alberto Bressan for his 60th birthday" guest edited by Fabio Ancona, Stefano Bianchini, Pierangelo Marcati, Andrea Marson.

Here, s is the saturation of the water phase, and c is the fraction of the polymer dissolved in the water phase. The function $f(s,c)$ denotes the fractional flow of water, normally taking the famous S-shaped Buckley–Leverett function [2]. The term $m(c)$ models the adsorption of polymer in the rock [10]. One usually assumes

$$m'(c) > 0, \qquad m''(c) < 0. \tag{1.2}$$

Letting $m(c)$=constant, (1.1) reduces to the simpler non-adsorptive model

$$\begin{cases} s_t + f(s,c)_x = 0, \\ (cs)_t + (cf(s,c))_x = 0. \end{cases} \tag{1.3}$$

We study the Riemann problems for (1.1) and (1.3), with initial data

$$(s,c)(0,x) = \begin{cases} (s^L, c^-), & \text{for } x < 0, \\ (s^R, c^+), & \text{for } x > 0. \end{cases} \tag{1.4}$$

We focus on the vanishing viscosity solutions and their dependence on the added viscosities.

The systems (1.1) and (1.3) are known to be parabolic degenerate along certain curves in the domain, where two eigenvalues and eigenvectors coincide. Along the degenerate curves, non-linear resonance occurs, and the total variation of the unknown $s(t,x)$ could blow up in finite time [9]. Analysis of this degenerate system is made feasible thanks to a decoupling feature of the system in a suitable Lagrangian coordinates [6,11]. One can define a Lagrangian coordinates (ψ, ϕ) as

$$\frac{\partial \phi}{\partial x} = -s, \quad \frac{\partial \phi}{\partial t} = f, \qquad \psi = x. \tag{1.5}$$

Here ϕ is the potential of the first equation in (1.1). In this Lagrangian coordinates, system (1.1) becomes triangular

$$\begin{cases} \dfrac{\partial}{\partial \phi}\left(\dfrac{s}{f(s,c)}\right) - \dfrac{\partial}{\partial \psi}\left(\dfrac{1}{f(s,c)}\right) = 0, \\ \dfrac{\partial}{\partial \phi} m(c) + \dfrac{\partial c}{\partial \psi} = 0. \end{cases} \tag{1.6}$$

In (1.6), the first equation describes the hydro-dynamics, while the second one denotes the thermo-dynamics. The decoupling feature in (1.6) indicates that the thermo-dynamics is independent of the hydro-dynamics. Thus, the solutions of c can be obtained independently by solving the second equation in (1.6). This possibly discontinuous solution can be plugged into the first equation and solve for s. This procedure leads to the consideration of a scalar conservation law with discontinuous flux. In the setting of the Riemann problem, the solution of c would contain a single jump. In the linear case where $m(c)$=constant, the c-jump is stationary in the Lagrangian coordinates. In the nonlinear case where $m(c)$ satisfies (1.2), the initial data $c^- > c^+$ results in a shock with speed

$$\sigma = \frac{m(c^-) - m(c^+)}{c^- - c^+}.$$

In a general setting, we consider a scalar conservation law with discontinuous flux

$$u_t + h(a(x), u)_x = 0, \tag{1.7}$$

where

$$a(x) = \begin{cases} a^- & (x < 0), \\ a^+ & (x > 0), \end{cases} \tag{1.8}$$

associated with initial Riemann data

$$u(0, x) = \begin{cases} u^L & (x < 0), \\ u^R & (x > 0). \end{cases} \tag{1.9}$$

The solutions to (1.7)–(1.9) can be obtained as limits of two combined approximations: (i) Approximating the jump function $a(\cdot)$ by a sequence of smooth functions $a_n(\cdot)$; (ii) Adding a viscosity term $\varepsilon_n u_{xx}$ on the right hand side of (1.7). In this setting, we consider the limits of approximations

$$u(t, x) = \lim_{n\to\infty} u^{(n)}(t, x)$$

where $u^{(n)}$ is a solution to the viscous conservation law with smooth flux

$$u_t + h(a_n(x), u)_x \; = \; \varepsilon_n u_{xx} \, . \tag{1.10}$$

We address the following three questions:

(1) For a given initial Riemann data, do the double limits $n \to \infty$ and $\varepsilon_n \to 0$ commute, or does the limit solution u depend on the relative rate at which the sequences $(1/n, \varepsilon_n)$ approach zero?
(2) If in general the limit solution depends on the ratio, what are the sufficient assumptions one can make such that all these limits are the same?
(3) How can one determine the traces $u^- = u(t, 0-), u^+ = u(t, 0+)$ in this limit solution?

In this paper we will show through several detailed counter examples that the double limits $n \to \infty$ and $\varepsilon_n \to 0$ do not commute. For the second question, we provide suitable monotonicity assumptions on the function $h(a, u)$ and the convergent sequence $a_n(x)$, such that the double limits are unique. The answer to the third question, worked out in a parallel paper [4], leads to a set of equivalent admissible conditions as well as a detailed construction of the solutions of Riemann problem, as the vanishing viscosity limit.

We remark that scalar conservation laws with discontinuous flux is a very active research field which has witnessed great progress in recent years. We refer to a survey paper [1] and references therein. A detailed discussion and list of references is beyond the scope of this paper.

We also consider a general triangular system of conservation laws

$$\begin{cases} u_t + h(\alpha, u)_x = 0, \\ \alpha_t + g(\alpha)_x = 0, \end{cases} \tag{1.11}$$

with initial data

$$\alpha(0,x) = \begin{cases} \alpha^- & (x<0), \\ \alpha^+ & (x>0), \end{cases} \qquad u(0,x) = \begin{cases} u^L & (x<0), \\ u^R & (x>0). \end{cases} \tag{1.12}$$

Let $\alpha = \alpha(t,x)$ be a solution to the second conservation law in (1.11), consisting of a single entropy-admissible shock with left and right states α^-, α^+, respectively. By performing a linear transformation of the t-x variables, we can assume that the shock speed is zero, so that $\alpha(t,x) = \alpha(0,x)$ for $t \geq 0$. Inserting this solution in the first equation one obtains (1.7).

We can now approximate (1.11) by the viscous system

$$\begin{cases} u_t + h(\alpha,u)_x = \varepsilon_n \, u_{xx}\,, \\ \alpha_t + g(\alpha)_x = \varepsilon_n' \, \alpha_{xx}\,. \end{cases} \tag{1.13}$$

Note that we allow the triangular system (1.11) to be parabolic degenerate. A natural question, also addressed in this paper, is whether the vanishing viscosity limit of (1.13) is uniquely determined, or it depends on the asymptotic ratio $\varepsilon_n/\varepsilon_n'$ at which the two diffusion coefficients approach zero.

Returning back to the Lagrangian system (1.6) for polymer flooding, the two parameters ε_n and ε_n' denote the viscosities for the hydro-dynamics and thermo-dynamics, respectively. Our discussions indicate that, the solution of the Riemann problem in general depends on the ratio of these two viscosities.

The rest of the paper is organized as follows. In Sect. 2 we recall the main results in [4]. These include three equivalent admissible conditions, and a Riemann solver that generates the vanishing viscosity solution. In Sect. 3 we provide a counter example showing that the Cauchy problem for (1.7), obtained as the vanishing viscosity limit in Sect. 2, does not depend continuously in $\mathbf{L}^1$ on the data $a(x)$. Several other detailed counter examples are constructed in Sect. 4, analytically and/or numerically, showing that infinitely many vanishing viscosity limits could be obtained for (1.10) and (1.13) by taking different ratios of $\varepsilon_n/\varepsilon_n'$. In Sect. 5 we introduce two monotonicity assumptions, and prove the uniqueness of the double limits under these assumptions. Finally, some concluding remarks are given in Sect. 6.

2. Review of admissibility conditions and Riemann solver for partially viscous model

We review the main results in the paper [4]. Consider the following partially viscous approximation to (1.7)

$$u_t + h(a(x),u)_x = \varepsilon_n u_{xx}, \tag{2.1}$$

where $a(x)$ is given in (1.8), and the equation is associated with Riemann data (1.9). For notation convenience, we denote the functions

$$h^-(u) \doteq h\left(a^-,u\right), \qquad h^+(u) \doteq h\left(a^+,u\right).$$

For any given u^L, u^R, we introduce the monotone functions

$$G^\sharp\left(u;u^R\right) \doteq \begin{cases} \max\left\{h^+(w);\ w\in[u^R,u]\right\}, & \text{if } u\ge u^R,\\ \min\left\{h^+(w);\ w\in[u,u^R]\right\}, & \text{if } u\le u^R, \end{cases} \tag{2.2}$$

$$G^\flat(u;u^L) \doteq \begin{cases} \min\left\{h^-(w);\ w\in[u^L,u]\right\}, & \text{if } u\ge u^L,\\ \max\left\{h^-(w);\ w\in[u,u^L]\right\}, & \text{if } u\le u^L. \end{cases} \tag{2.3}$$

We assume that, for the given data u^L, u^R, there exists some $\tilde u^*$ such that

$$G^\flat\left(\tilde u^*;u^L\right) = G^\sharp\left(\tilde u^*;u^R\right). \tag{2.4}$$

The following Theorem, proved in [4], states three equivalent admissible conditions for the jump at $x=0$.

Theorem 2.1. *Given (u^-,u^+), let $a(x)$ be the jump function in (1.8), and let $\hat u$ be the jump function*

$$\hat u(x) \doteq \begin{cases} u^- & (x<0),\\ u^+ & (x>0). \end{cases} \tag{2.5}$$

The following three conditions are equivalent.

(I) *There exists a family of monotone viscous solutions $u^\varepsilon(t,x)$ of (2.1) such that*

$$\lim_{\varepsilon\to 0+}\|u^\varepsilon(t,\cdot)-\hat u(\cdot)\|_{\mathbf{L}^1}=0, \tag{2.6}$$

uniformly on every bounded time interval $[0,T]$.

(II) *The following Rankine–Hugoniot condition holds*

$$h^-(u^-)=h^+(u^+)\doteq \bar h \tag{2.7}$$

together with the following generalized Oleinik-type conditions:

(i) *If $u^-<u^+$, then there exists an intermediate state $u^*\in[u^-,u^+]$ such that*

$$\begin{cases} h^-(u)\ge \bar h & \text{for } u\in\left[u^-,u^*\right],\\ h^+(u)\ge \bar h & \text{for } u\in\left[u^*,u^+\right]. \end{cases} \tag{2.8}$$

(ii) *If $u^->u^+$, then there exists an intermediate state $u^*\in[u^+,u^-]$ such that*

$$\begin{cases} h^+(u)\le \bar h & \text{for } u\in\left[u^+,u^*\right],\\ h^-(u)\le \bar h & \text{for } u\in\left[u^*,u^-\right]. \end{cases} \tag{2.9}$$

(III) *There exists a state $\tilde u^*$, between u^- and u^+, such that*

$$\bar h = h^-(u^-) = G^\flat\left(\tilde u^*;u^-\right) = G^\sharp\left(\tilde u^*;u^+\right) = h^+\left(u^+\right). \tag{2.10}$$

Condition (III) leads to a Riemann solver, which generates vanishing viscosity solutions of (2.1) as $\varepsilon_n\to 0+$, proved in [4]. See also an earlier work [3]

Theorem 2.2. *Given a left and right states* (u^L, u^R), *let* $G^\sharp(u; u^R), G^\flat(u; u^L)$ *be defined as in* (2.2)–(2.3), *and let* $\bar{h}$ *be the unique value such that*

$$\bar{h} = G^\flat\left(\tilde{u}^*; u^L\right) = G^\sharp\left(\tilde{u}^*; u^R\right) \tag{2.11}$$

for some $\tilde{u}^*$. *We define the trace* u^-, u^+ *of* u *along* $x = 0$ *as follows:*

$$u^- \doteq \operatorname{argmin}\left\{\left|u - u^L\right|;\, h^-(u) = \bar{h}\right\}, \tag{2.12}$$

$$u^+ \doteq \operatorname{argmin}\left\{\left|u - u^R\right|;\, h^+(u) = \bar{h}\right\}. \tag{2.13}$$

Then, the vanishing viscosity solution $u(t,x)$ *of* (1.7)–(1.9) *is obtained by piecing together the solutions to*

$$u_t + h^-(u)_x = 0, \qquad u(0,x) = \begin{cases} u^L, & \text{if } x < 0, \\ u^-, & \text{if } x > 0, \end{cases} \tag{2.14}$$

for $x < 0$, *and the solution to*

$$u_t + h^+(u)_x = 0, \qquad u(0,x) = \begin{cases} u^+, & \text{if } x < 0, \\ u^R, & \text{if } x > 0, \end{cases} \tag{2.15}$$

for $x > 0$. *In particular, for every* $t > 0$ *we have*

$$\lim_{x \to 0-} u(t,x) = u^-, \qquad \lim_{x \to 0+} u(t,x) = u^+, \tag{2.16}$$

and

$$\lim_{\varepsilon \to 0} \|u^\varepsilon(t,\cdot) - u(t,\cdot)\|_{\mathbf{L}^1(\mathbb{R})} = 0 \tag{2.17}$$

uniformly on every bounded time interval $[0,T]$, *where* u^ε *is a solution to the viscous equation* (2.1) *with the same initial data.*

3. Lack of continuous dependence on the coefficient $a(x)$

We present a counter example which shows that the solution $u(t,x)$ of the Cauchy problem (1.7)–(1.9), defined as the vanishing viscosity solution of the partially viscous model (2.1), does not depend continuously on the coefficient $a(x)$ in $\mathbf{L}^1$. The example consists of two Riemann problems, whose unique solutions are constructed as the vanishing viscosity solutions in Theorem 2.2.

Example 3.1. *Consider the Cauchy problem for* (1.7) *with*

$$a(x) = a^\ell(x) \doteq \begin{cases} a_1 & \text{if } |x| < \ell, \\ a_2 & \text{if } |x| > \ell, \end{cases}$$

with $a_1 < a_2$, *and denote the flux functions as*

$$h_1(u) \doteq h(a_1, u), \qquad h_2(u) \doteq h(a_2, u).$$

We consider constant initial data $u(0,x) = \tilde{u}$. *Assume the functions* h_1, h_2 *and data* $\tilde{u}$ *are as illustrated in Fig. 1 (left plot), where* $\tilde{u}$ *is the point where* $h_1(\cdot)$ *reaches its maximum.*

The solution of this Cauchy problem consists of two Riemann problem solutions, at $x = \pm\ell$. *At* $x = -\ell$, *the solution consists of a u-shock from* A *to* D *with negative speed, and a stationary a-jump from* D *to* C. *At* $x = \ell$, *the*

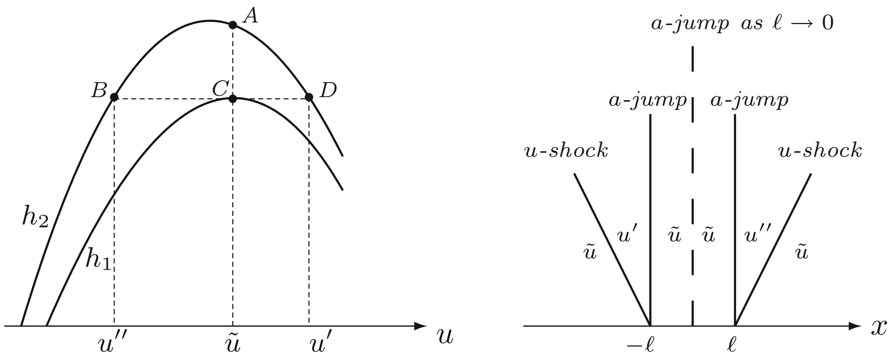

Figure 1. Solution consists of patching together two Riemann problems

Riemann solution consists of a stationary a-jump from C to B, and a u-shock from B to A, with positive speed. See Fig. 1*.*

In the limit, as $\ell \to 0$*, the two a-jumps merge into one single jump at* $x = 0$*, where* a *is continuous, and* u *takes* u' *and* u'' *as the left and right limits. This jump is not entropy admissible.*

Note that, this limit solution is not the solution with the function $a(x) = a_2$*, which would have given the trivial constant solution* $u(t, x) = \tilde{u}$*.*

Remark 3.2. We observe that the lack of continuous dependence is caused by the fact that, as the sequence $a^\ell(x)$ converges to the constant function a_2 in $\mathbf{L}^1$, the total variation does not converge, i.e., the function $a^\ell(x)$ is not monotone. At first glance this counter example seems rather irrelevant to our discussion on solutions of a single Riemann problem. However, this non-monotonicity actually serves as the key ingredient in one of our counter examples in Sect. 4.1, where the non-monotonicity is built into the flux function itself. Then we can construct infinitely many vanishing viscosity limits for (1.10).

4. Non-uniqueness of the double vanishing viscosity limits

In this section we construct several counter examples for various cases.

4.1. Scalar conservation laws with discontinuous flux functions

We consider the Riemann problem (1.7)–(1.9). Let $u_{\varepsilon,n}$ be the solutions for the approximate viscous model

$$u_t + h(a_n(x), u)_x \;=\; \varepsilon u_{xx}, \tag{4.1}$$

where a_n are smooth and monotone functions that converges to $a(x)$. We will show that, in many cases, one has

$$\lim_{n\to\infty} \lim_{\varepsilon\to 0+} u_{\varepsilon,n} \;\neq\; \lim_{\varepsilon\to 0+} \lim_{n\to\infty} u_{\varepsilon,n}. \tag{4.2}$$

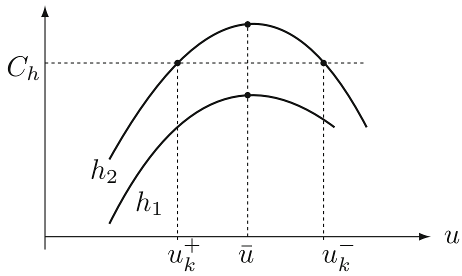

FIGURE 2. The functions h_1, h_2 and the values of $u_\kappa^\pm$

Let $h_1(\cdot), h_2(\cdot)$ be two concave functions with $h_1(u) < h_2(u)$ for all u. Let $\bar{u}$ be the point where both $h_1(\cdot)$ and $h_2(\cdot)$ attain the maximum value, see Fig. 2. Let $a^- < a^+$, and let $a^m = (a^- + a^+)/2$ be the mid-point.

For $a \in (a^-, a^+)$, let the flux function $h(a, u)$ be defined as

$$h(a,u) = \begin{cases} \dfrac{a^m - a}{a^m - a^-} h_2(u) + \dfrac{a - a^-}{a^m - a^-} h_1(u), & \text{if } a^- < a < a^m. \\ \dfrac{a^+ - a}{a^+ - a^m} h_1(u) + \dfrac{a - a^m}{a^+ - a^m} h_2(u), & \text{if } a^m < a < a^+. \end{cases} \tag{4.3}$$

Then we clearly have

$$h(a^-, u) = h(a^+, u) = h_2(u), \qquad h(a^m, u) = h_1(u).$$

Note that the partial derivative $\partial h/\partial a$ changes sign at $a = a^m$.

Consider the Riemann problem (1.7)–(1.9) with the Riemann data

$$u^L = u^R = \bar{u}. \tag{4.4}$$

Since we have $h^- = h^+$, the solution to this Riemann problem is trivially the constant function $u(t,x) \equiv \bar{u}$ for all (t,x). However, we will show that, for the approximate model (4.1), the case is quite different.

Consider a sequence $a_n(x)$, smooth and monotone, satisfying

$$a_n(x) \doteq \bar{a}(nx), \qquad \bar{a}(\xi) \doteq \begin{cases} a^- & \text{if } \xi < -2, \\ a^m & \text{if } -1 < \xi < 1, \\ a^+ & \text{if } \xi > 2. \end{cases} \tag{4.5}$$

We have now

$$\lim_{n\to\infty} a_n(x) = a(x). \tag{4.6}$$

For each given a_n, we seek a stationary viscous profile $u(t,x) = U(x)$ for (4.1). Such a profile, if exists, must satisfy the ODE

$$\varepsilon U' = h\left(a_n(x), U\right) - C_h, \tag{4.7}$$

where

$$C_h = h\left(a^-, U(-\infty)\right) = h\left(a^+, U(+\infty)\right), \tag{4.8}$$

for some suitable $U(\pm\infty)$ which will be determined later.

Let ε_n be a sequence of viscosity such that $\varepsilon_n \to 0$ as $n \to \infty$ with a fixed ratio κ, i.e.,

$$\varepsilon_n \doteq \kappa/n, \qquad \kappa = n\varepsilon_n. \tag{4.9}$$

We now study in detail the rescaled ODE, with $\xi \doteq nx$,

$$\kappa \cdot U'(\xi) = h\left(\bar{a}(\xi), U(\xi)\right) - C_h. \tag{4.10}$$

We claim that, there exists a value κ_M, such that the followings hold.

(i) For every $\kappa \in [0, \kappa_M)$, there exists a unique value $C_h \in [h_1(\bar{u}), h_2(\bar{u}))$, such that the ODE (4.10) has a unique monotone solution $U_\kappa(\cdot)$, with

$$U_\kappa(-\infty) = u_\kappa^-, \quad U_\kappa(+\infty) = u_\kappa^+,$$

where u_κ^-, u_κ^+ are the unique values that satisfy (see Fig. 2)

$$h_2(u_\kappa^-) = h_2(u_\kappa^+) = C_h, \qquad u_\kappa^- > \bar{u} > u_\kappa^+.$$

(ii) For $\kappa \geq \kappa_M$, we have $C_h = h_2(\bar{u})$, and the unique solution for the ODE (4.10) is the constant function $U_\kappa(\xi) = \bar{u}$.

If these claims hold, then the functions

$$u^{\kappa,\varepsilon_n}(t,x) = U_\kappa(x/\varepsilon_n)$$

provide a stationary traveling wave solution to the viscous conservation law (4.1), with boundary conditions

$$u^{\kappa,\varepsilon}(t, \pm\infty) = u_\kappa^\pm.$$

In addition, we consider a sequence of solutions v_n to the viscous Riemann problems

$$v_t + h(a^-, v)_x = \varepsilon_n v_{xx}, \qquad v(0,x) = \begin{cases} \bar{u}, & (x < 0), \\ u_\kappa^-, & (x > 0), \end{cases}$$

and a sequence of solutions w_n to the viscous Riemann problems

$$w_t + h(a^+, w)_x = \varepsilon_n w_{xx}, \qquad w(0,x) = \begin{cases} u_\kappa^+, & (x < 0), \\ \bar{u}, & (x > 0). \end{cases}$$

Note that if $\bar{u} \neq u_\kappa^\pm$, v_n contains only viscous traveling waves with negative speed, while w_n with positive speed. Patching together the functions $v_n, u^{\kappa,\varepsilon_n}, w_n$, in a similar way as in the proof for Theorem 2.2 in [4], we can construct a sequence of solutions to (4.1) with Riemann data (u^L, u^R) where $u^L = u^R = \bar{u}$, converging to a self-similar limit function $u^\kappa(t,x) = U^\kappa(x/t)$ with the following properties. For $x < 0$, u^κ provides the entropy solution to the Riemann problem

$$u_t + h(a^-, u)_x = 0, \qquad u(0,x) = \begin{cases} \bar{u}, & (x < 0), \\ u_\kappa^-, & (x > 0). \end{cases}$$

For $x > 0$, u^κ provides the entropy solution tot he Riemann problem

$$u_t + h(a^+, u)_x = 0, \qquad u(0,x) = \begin{cases} u_\kappa^+, & (x < 0), \\ \bar{u}, & (x > 0). \end{cases}$$

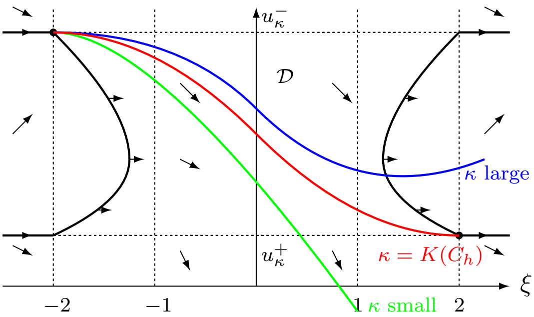

FIGURE 3. Illustration for the vector field of $u'(s)$, and some sample solutions of the ODE (4.10) for a given C_h and for various values of κ

It is then clear that infinitely many different limits can be obtained, by choosing different values of the ratio κ.

We now prove these claims.

Proof. The proof takes several steps.
Step 1 We first show that, for every given $C_h \in (h_1(\bar{u}), h_2(\bar{u}))$, there exists a unique κ such that the ODE (4.10) has a unique solution that satisfies the claim (i).

Indeed, by the continuity of the function $h(a, u)$, there exists a continuous function $\mathcal{X}(u)$ on $u_\kappa^+ < u < u_\kappa^-$ with $1 < \mathcal{X} < 2$ such that the right hand side of the ODE (4.10) is 0 along the curves $\xi = \pm\mathcal{X}(u)$ for $u_\kappa^+ < u < u_\kappa^-$. See the black curves in Fig. 3. Define the domain

$$\mathcal{D} = \left\{(\xi, u) : u_\kappa^+ < u < u_\kappa^-,\ -\mathcal{X}(u) < \xi < \mathcal{X}(u)\right\}.$$

We have

$$\kappa u'(\xi) : \begin{cases} <0, & (\xi, u) \in \mathcal{D}, \\ <0, & u > u_\kappa^- \text{ or } u < u_\kappa^+, \\ >0, & \text{otherwise.} \end{cases}$$

Let the ODE (4.10) have the initial condition $u(\xi) = u_\kappa^-$ for $\xi \le -2$, and consider the solution at $\xi = 2$. By the comparison principle and the uniqueness of the solution of the ODE, $u_\kappa(2)$ changes continuously and monotonely in κ. In fact, for sufficiently large value of κ we have $u_\kappa(2) > u_\kappa^+$, so the solution $u_\kappa(\xi) \to u_\kappa^-$ as $\xi \to +\infty$. For sufficiently small κ, we have $u_\kappa(2) < u_\kappa^+$, and the solution $u_\kappa(\xi) \to -\infty$ as $\xi \to +\infty$. By continuity we conclude that, for each given C_h, there exists a unique value of κ such that $u_\kappa(\xi) = u_\kappa^+$ for $\xi \ge 2$. See Fig. 3 for sketches of these three typical solutions. We denote this mapping by $\kappa = K(C_h)$.
Step 2 There are two limit cases. First, if $C_h = h_2(\bar{u})$, we denote the limit value as $\kappa_M = K(h_2(\bar{u}))$. In this case, we have $u_\kappa^- = u_\kappa^+ = \bar{u}$, and the traveling wave is a constant function. Second, if $C_h = h_1(\bar{u})$, the righthand side of (4.10) is

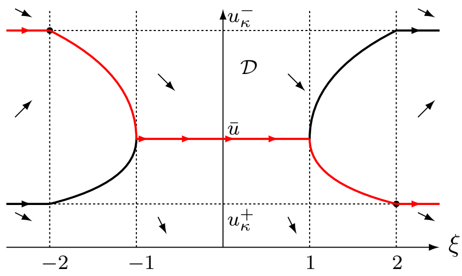

FIGURE 4. The limit case with $C_h = h_1(\bar{u})$ and $\kappa = 0$. The solution path (indicated in *red*) goes through curves where the vector field $\kappa u'(\xi) = 0$

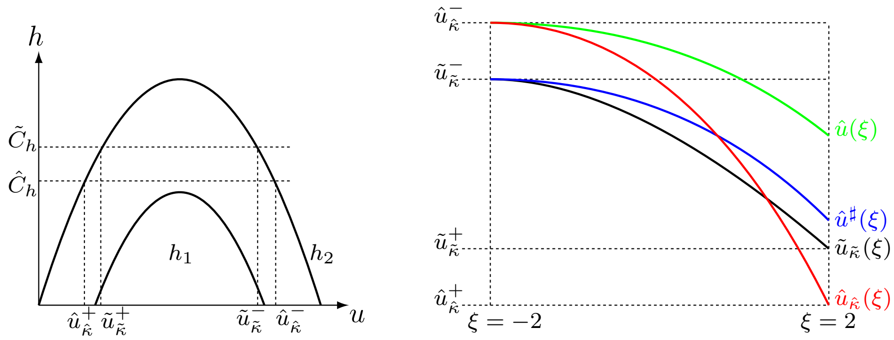

FIGURE 5. The monotonicity of the mapping $\kappa = K(C_h)$: $\hat\kappa < \tilde\kappa$ if and only if $\hat{C}_h < \tilde{C}_h$

zero on the line segment with $u = \bar{u}$ and $-1 \le \xi \le 1$ in the domain $\mathcal{D}$, and the end points of the segment connect to the boundary of $\mathcal{D}$. In this case, the only possible path from u_κ^- to u_κ^+ is when $\kappa = 0$, and the path goes through the curve where $h(\alpha(\xi) - u(\xi)) - C_h = 0$. See Fig. 4.

Step 3 In order to show that there exists a distinct value of C_h for each given $0 \le \kappa \le \kappa_M$, it suffices to show that the mapping $\kappa = K(C_h)$ is monotone increasing and therefore one-to-one. Let $\tilde{C}_h, \hat{C}_h, \tilde\kappa, \hat\kappa$ be given such that

$$\tilde\kappa = K(\tilde{C}_h), \qquad \hat\kappa = K(\hat{C}_h), \qquad h_1(\bar{u}) < \hat{C}_h < \tilde{C}_h < h_2(\bar{u}).$$

We need to establish the relation

$$\hat\kappa < \tilde\kappa. \tag{4.11}$$

Indeed, the situation is illustrated in Fig. 5, and the proof depends on a topological argument. Let $\tilde{u}_{\tilde\kappa}(\xi)$ be the unique solution to the ODE

$$u'(\xi) = \tilde\kappa^{-1} \cdot \left[h(a(\xi), u(\xi)) - \tilde{C}_h\right] \tag{4.12}$$

which satisfies the following

$$\tilde{u}_{\tilde{\kappa}}(-2) = \tilde{u}^-_{\tilde{\kappa}}, \quad \tilde{u}_{\tilde{\kappa}}(2) = \tilde{u}^+_{\tilde{\kappa}}, \quad h_2(\tilde{u}^-_{\tilde{\kappa}}) = h_2(u^+_{\tilde{\kappa}}) = \tilde{C}_h, \quad \tilde{u}^-_{\tilde{\kappa}} > \tilde{u}^+_{\tilde{\kappa}}.$$

Let $\hat{u}^\sharp(\xi)$ be the solution of the ODE

$$u'(\xi) = \tilde{\kappa}^{-1} \cdot \left[h(\alpha(\xi), u(\xi)) - \hat{C}_h\right], \qquad \hat{u}^\sharp(-2) = \tilde{u}^-_{\tilde{\kappa}}. \tag{4.13}$$

Since the right hand side of (4.13) is strictly larger than that of (4.12), by a standard comparison argument we have $\hat{u}^\sharp(2) > \tilde{u}_{\tilde{\kappa}}(2)$.

Define $\hat{u}^-_{\hat{\kappa}}, \hat{u}^+_{\hat{\kappa}}$ as the unique values such that

$$h_2(\hat{u}^-_{\hat{\kappa}}) = h_2(\hat{u}^+_{\hat{\kappa}}) = \hat{C}_h, \qquad \hat{u}^-_{\hat{\kappa}} > \hat{u}^+_{\hat{\kappa}}.$$

Then, by the properties of $h(a, u)$ (see the left plot in Fig. 5) we have

$$\hat{u}^-_{\hat{\kappa}} > \tilde{u}^-_{\tilde{\kappa}} > \tilde{u}^+_{\tilde{\kappa}} > \hat{u}^+_{\hat{\kappa}}.$$

Let $\hat{u}(\xi)$ be the unique solution of the ODE (4.13) with initial condition $\hat{u}(-2) = \hat{u}^-_{\hat{\kappa}}$. By the uniqueness of solutions we have

$$\hat{u}(2) > \hat{u}^\sharp(2) > \tilde{u}_{\tilde{\kappa}}(2) > \hat{u}^+_{\hat{\kappa}}.$$

See the right plot in Fig. 5. Finally, let $\hat{u}_{\hat{\kappa}}(\xi)$ be the solution of the ODE

$$u'(\xi) = \hat{\kappa}^{-1} \cdot \left[h(\alpha(\xi), u(\xi) - \hat{C}_h\right],$$

which satisfies

$$\hat{u}_{\hat{\kappa}}(-2) = \hat{u}^-_{\hat{\kappa}}, \quad \hat{u}_{\hat{\kappa}}(2) = \hat{u}^+_{\hat{\kappa}}, \quad h_2(\hat{u}^-_{\hat{\kappa}}) = h_2(\hat{u}^+_{\hat{\kappa}}) = \hat{C}_h, \quad \hat{u}^-_{\hat{\kappa}} > \hat{u}^+_{\hat{\kappa}}.$$

The above analysis indicates that this is only possible when $\hat{\kappa} < \tilde{\kappa}$, proving (4.11).

Step 4 Finally, if $\kappa > \kappa_M$, the monotonicity of the mapping K implies $C_h \geq h_2(\bar{u})$. However, if $C_h > h_2(\bar{u})$, then the right hand side of the ODE (4.10) will be strictly negative for all ξ, and no bounded traveling wave exists. Thus, we must have $C_h = h_2(\bar{u})$, which implies $u^\pm_\kappa = \bar{u}$, and the constant function $U_\kappa(\xi) = \bar{u}$ is the unique solution. □

Remark 4.1. We observe that, for $\kappa < \kappa_M$, the vanishing viscosity solution of (4.1) contains a stationary downward jump at $x = 0$, from u^-_κ to u^+_κ. This jump is not entropy admissible for the conservation law

$$u_t + h_2(u)_x = 0$$

which is the equation for the limit as $n \to \infty$.

4.2. Triangular systems

Example 4.2. *We now consider the triangular system* (1.11) *with Riemann data* (1.12)*. Without loss of generality, we assume that* $g(\alpha^-) = g(\alpha^+) = 0$ *and* $g(\alpha) > 0$ *for all* $\alpha \in (\alpha^-, \alpha^+)$*, such that the upward jump in* α *is admissible and stationary. Let* $\alpha^m = \frac{1}{2}(\alpha^- + \alpha^+)$*, and let the function* $h(\alpha, u)$ *be defined as* (4.3)*. We consider the Riemann problem with* $u^L = u^R = \bar{u}$*, where* $\bar{u}$ *is the point where both* h_1, h_2 *attain the maximum.*

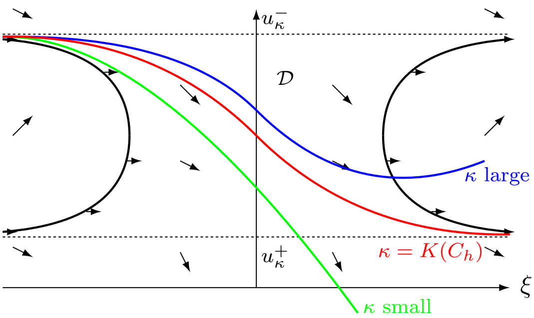

Figure 6. For the *triangular* system: illustration for the vector field of $\kappa u'(s)$, and some sample solutions of the ODE (4.16) for a given C_h and for various values of κ

Consider the corresponding viscous system (1.13).

$$\begin{cases} u_t + h(\alpha, u)_x = \varepsilon_n u_{xx}, \\ \alpha_t + g(\alpha)_x = \varepsilon'_n \alpha_{xx} . \end{cases} \tag{4.14}$$

Denote the ratio $\kappa \doteq \varepsilon_n/\varepsilon'_n$, *and let* $(u^{\varepsilon_n, \varepsilon'_n}, \alpha^{\varepsilon'_n})$ *be the viscous solutions for* (4.14). *The solution* $\alpha^{\varepsilon'_n}$ *is a stationary viscous traveling wave which is smooth and monotone, connecting the two states* α^- *and* α^+.

Let $U(\xi), A(\xi)$ *be the rescaled stationary traveling wave solution for* (4.14), *with* $\xi = x/\varepsilon'_n$. *Then, they must satisfy the ODEs*

$$\begin{cases} A'(\xi) = g(A(\xi)), \\ \kappa U'(\xi) = h(A(\xi), U(\xi)) - C_h, \end{cases} \tag{4.15}$$

with the boundary conditions $A(\pm\infty) = a^\pm$, *and*

$$C_h = h(A(-\infty), U(-\infty)) = h(A(+\infty), U(+\infty)).$$

Without loss of generality, we may set $A(0) = \alpha^m$.

Much of the analysis in the example in Sect. 4.1 *can be carried out in an analogous way. The function* $\mathcal{X}(u)$ *is modified, which is a smooth function with asymptotes at* $u = u_\kappa^\pm$, *see Fig.* 6. *The solution of the ODE*

$$\kappa U'(\xi) = h(A(\xi), U(\xi)) - C_h, \qquad U(-\infty) = u_\kappa^- \tag{4.16}$$

is defined in the following limiting process. Let $\{\hat{u}_n\}$ *be a convergent sequence such that* $\lim_{n\to\infty} \hat{u}_n = u_\kappa^-$. *Consider point* $(\hat{\xi}, \hat{u}_n)$ *with* $\hat{\xi} = -\mathcal{X}(\hat{u}_n)$, *on the left black curve in Fig.* 6. *Let* U_n *be the unique solution to the ODE*

$$\kappa U'(\xi) = h(A(\xi), U(\xi)) - C_h, \qquad U(\hat{\xi}) = \hat{u}_n. \tag{4.17}$$

The solution for (4.16) *is then the unique limit* $U_n(\xi)$ *as* $n \to \infty$. *The rest of the example follows.*

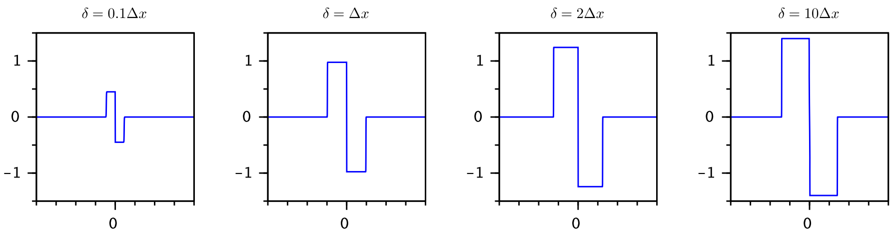

FIGURE 7. Simulation results for Example 4.3

4.3. Counter examples by numerical simulations

All numerical simulations are performed using Scilab. To access all the codes used for the examples in this paper, see [8].

Example 4.3. *We simulate the counter example in Sect. 4.1. We consider the conservation law*

$$u_t + h(a,u)_x = 0, \qquad h(a,u) = 2a^2 - u^2, \qquad a(x) = \bar{a}(x/\delta),$$

and the function $\bar{a}(\xi)$ *with* $\xi = x/\delta$ *is (see (4.5))*

$$\bar{a}(\xi) \doteq \begin{cases} 0 & \text{if } 0 < \xi < 1, \\ \xi - 1 & \text{if } 1 < \xi < 2, \\ 1 & \text{if } \xi > 2, \end{cases} \qquad \text{and} \qquad \bar{a}(-\xi) = -\bar{a}(\xi).$$

Lax Friedrich method is used, which adds numerical diffusion to the equation. Thus, varying the ratio $\delta/\Delta x$ *here has a similar effect as varying the ratio* κ *in the example in Sect. 4.1. We use the Riemann data* $u^L = u^R = 0$*, and simulate with* $\delta/\Delta x = 0, 0.1, 1, 2, 10$ *with final computing time* $T = 0.1$*. For* $\delta = 0$*, the solution is the constant function* $u(x) = 0$*. The plots of the solutions for the other 4 values of* $\delta/\Delta x$ *are shown in Fig. 7. These are exactly as predicted in the Example of Sect. 4.1.*

Example 4.4. *In this example we provide another counter example that has multiple double limits, first through numerical simulations, then follow up with some analysis. Consider*

$$u_t + h(a,u)_x = 0, \qquad h(a,u) = -(u - 2 - 3a)^2,$$

where

$$a(x) = \begin{cases} 0 & (x < -\delta), \\ x/(2\delta) & (-\delta < x < \delta), \\ 1 & (x > \delta). \end{cases}$$

We use the Riemann data $u^L = 3, u^R = 4$*, and simulate using Lax–Friedrich method, for* $\delta/\Delta x = 0, 1, 5, 100$*, with* $T = 0.1$*. Simulation results are shown in Fig. 8 (top). Clearly, different values of* $\delta/\Delta x$ *give different paths of Riemann*

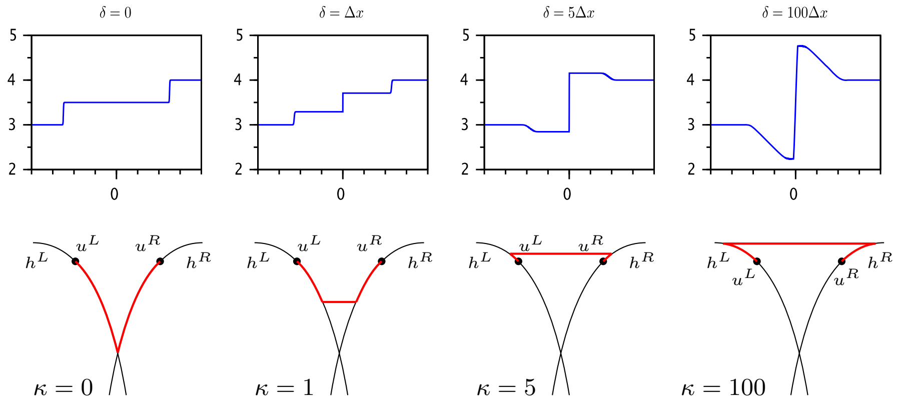

FIGURE 8. Simulation results (*top*) and paths (*bottom*) of Riemann solutions for Example 4.4

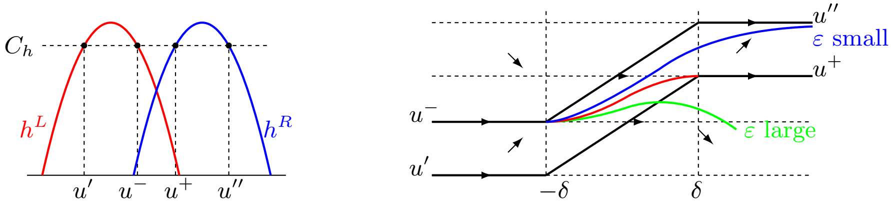

FIGURE 9. Vector field and solution paths for Example 4.4

solutions. These paths are shown in Fig. 8 *(bottom) in the graphs for the flux functions*

$$h^L(u) = h(0,u) = -(u-2)^2, \qquad h^R(u) = h(1,u) = -(u-5)^2.$$

A detailed analysis of this example, similar to the analysis in Sect. 4.1*, can be carried out. We briefly explain the highlights here and omit some details. Consider the viscous equation*

$$u_t + h(a(x),u)_x = \varepsilon u_{xx}.$$

Stationary traveling waves $U^{\varepsilon,\delta}(x)$ *connecting* u^-, u^+ *must satisfy the ODE:*

$$\varepsilon U' = h(a(x),U) - C_h, \quad C_h = h^L(u^-) = h^R(u^+), \quad U(\pm\infty) = u^{\pm\infty}. \quad (4.18)$$

The vector field for U' *and some sample solutions are illustrated in Fig.* 9*. It shows that, for each* C_h *and* δ*, there exists an* ε*, such that there exists a monotone solution that connects* u^- *to* u^+ *(the red curve in Fig.* 9*). In the limit case where* $\delta = 0$*, the only possible solution that connects* u^- *to* u^+ *is when* $u^- = u^+$*, i.e., the intersection point of the graphs* $h^L(u)$ *and* $h^R(u)$*. This coincides with the results in Theorems* 2.1 *and* 2.2*.*

4.4. Counter examples for polymer flooding models

Applying Theorems 2.1 and 2.2 to the polymer flooding system has lead to a Riemann solver (used in [7]), as the vanishing viscosity limit [4]. Furthermore, the application of the counter examples in Sects. 4.1 and 4.2 to the polymer flooding model (1.1) is also apparent for the systems in the Lagrangian coordinate (1.6). The equivalence of weak solutions between the Eulerian and Lagrangian coordinates is proved in a seminal paper of Wagner [11], under the assumption that $s > 0$.

Unfortunately, translating the viscosities in the Lagrangian coordinates back to Eulerian coordinates leads to very complicated equations. From the modeling point of view, one may consider the following approximation

$$\begin{cases} s_t + f(s,c)_x = \varepsilon_1 s_{xx}, \\ (m(c) + sc)_t + (cf(s,c))_x = \varepsilon_1 (cs_x)_x + \varepsilon_2 (m(c)_x + sc_x)_x. \end{cases} \tag{4.19}$$

Intuitively, ε_1 and ε_2 denote the viscosities for s and c, respectively.

We conjecture that:

(i) For traveling waves, the vanishing viscosity solution of (4.19) is equivalent to the triangular system (1.6) in Lagrangian coordinate;
(ii) For Cauchy problems, the vanishing viscosity solution of (4.19) is also equivalent to the triangular system (1.6) in Lagrangian coordinate.

Conjecture (i) can be simply confirmed by analyzing the ODEs satisfied by the traveling waves. For conjecture (ii), utilizing method of characteristics, it leads to the study of a parabolic equation. Aspects of these claims would be studied in a future work.

In this paper we present a numerical study, where different double limits are achieved.

Example 4.5. *Consider the non-adsorptive model* (1.3) *and consider the flux*

$$f(s,c) = \frac{s^2}{s^2 + a(c)(1-s)^2}, \qquad \textit{where} \quad a(c) = 1 - 4(c-0.5)^2.$$

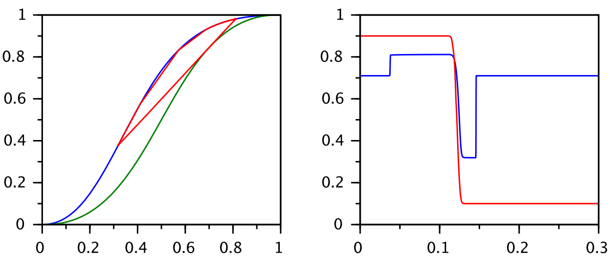

FIGURE 10. Simulation results for Example 4.5. *Left*: graph of f^L, f^R in *blue*, f^M in *green*, and the path of Riemann solution in *red*. *Right*: Solution s (*blue*) and c (*red*) (colour figure online)

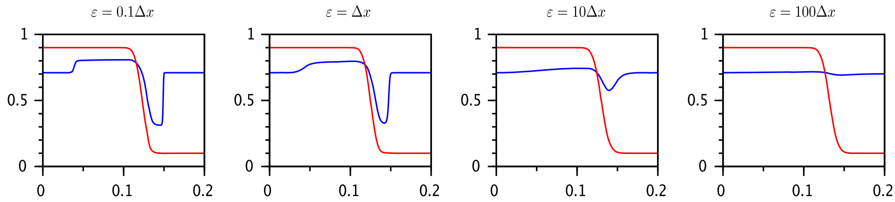

FIGURE 11. Simulation results for Example 4.6. Here the solution s is plotted in *blue* and c in *red*

Note that the function $a(c)$ is not monotone, causing the mapping $c \mapsto f(s,c)$ to be non monotone. We use the following Riemann data

$$s^L = 0.71, \quad c^L = 0.9, \qquad s^R = 0.71, \quad c^R = 0.1.$$

In this setting, we have

$$f^L(s) \doteq f(s,c^L) = f^R(s) \doteq f(s,c^R),$$

but for mid value $c^M = (c^L + c^R)/2$, the flux $f^M(s) = f(s,c^M)$ is different. See Fig. 10 (left).

Since all wave speeds are positive, upwind method is used, which adds small amount of numerical viscosities to both s and c. The simulation results at $T = 0.1$ are plotted in Fig. 10 (right).

Using the Riemann solver in [4], one obtains the constant solution $s = 0.71$. However, our numerical solution is very different. The result here suggests the existence of multiple double limits of (4.19), as $\varepsilon_1, \varepsilon_2 \to 0$ at different rate. Details are shown in the next Example.

Example 4.6. *In the same setting as Example 4.5, we consider the viscous approximation*

$$\begin{cases} s_t + f(s,c)_x = \varepsilon s_{xx}, \\ (sc)_t + (cf(s,c))_x = \varepsilon(cs_x)_x. \end{cases}$$

Since upwind method adds numerical diffusions to both equations, varying the ratio $\varepsilon/\Delta x$ here has a similar effect as varying the ratio $\varepsilon_1/\varepsilon_2$ for the following system

$$\begin{cases} s_t + f(s,c)_x = \varepsilon_1 s_{xx}, \\ (sc)_t + (cf(s,c))_x = \varepsilon_1(c \cdot s_x)_x + \varepsilon_2(s \cdot c_x)_x. \end{cases}$$

Simulation results are plotted in Fig. 11, for various ε values. We observe that, for larger values of $\varepsilon/\Delta x$, the numerical solution approaches the constant solution $s(t,x) = 0.71$.

5. Uniqueness of the vanishing viscosity limit

5.1. Scalar conservation laws with discontinuous flux

We consider again the Riemann problem for conservation law with discontinuous flux (1.7)–(1.9). In this setting, Theorem 2.2 describes the unique solution which is obtained as the limit of vanishing viscosity approximation u^ε in (2.1). The counter examples in Sect. 4 show that this solution doesn't need to coincide with a limit of more general approximations of the form (4.1). In this section we prove sufficient conditions in order that the approximations in (4.1) all converge to the the same limit solution.

Toward this goal, two monotonicity assumptions are needed.

(M1) For every u, the function $a \mapsto h(a,u)$ is monotone. Namely, either $\dfrac{\partial h}{\partial a}(a,u) \geq 0$ or $\dfrac{\partial h}{\partial a}(a,u) \leq 0$ for all a, u.

(M2) The functions a_n are smooth and converge to the jump function $a(x)$ in (1.8) in the $\mathbf{L}^1$ distance. Moreover, they are all monotone:

$$\begin{array}{lcll} a^- \leq a^+ & \Longrightarrow & a_n'(x) \;\geq\; 0 & \forall x, n\,, \\ a^- \geq a^+ & \Longrightarrow & a_n'(x) \;\leq\; 0 & \forall x, n\,. \end{array}$$

We note that, the condition **(M1)** indicates that, for two distinct values of a_1, a_2, the graphs of $u \mapsto h(a_1,u)$ and $u \mapsto h(a_2,u)$ will ever crossing each other.

Theorem 5.1. *In the same setting as Theorem 2.1, let u^-, u^+ be two states which satisfy the admissibility conditions, and call $\hat{u}$ the jump function in (2.5). Let $u_n = u_n(t,x)$ be a sequence of solutions to the viscous conservation laws*

$$u_t + h(a_n(x), u)_x = \varepsilon_n u_{xx}, \tag{5.1}$$

where

$$\lim_{n\to\infty} \varepsilon_n = 0, \qquad \lim_{n\to\infty} a_n(x) = a(x).$$

Assume that the initial data of (5.1) satisfies

$$\lim_{n\to\infty} \|u_n(0,\cdot) - \hat{u}(\cdot)\|_{\mathbf{L}^1} = 0. \tag{5.2}$$

*If the monotonicity assumptions (**M1**)–(**M2**) are satisfied, then*

$$\lim_{n\to\infty} \|u_n(\tau,\cdot) - \hat{u}(\cdot)\|_{\mathbf{L}^1} \;=\; 0, \tag{5.3}$$

uniformly as τ ranges in bounded sets.

Proof. We first observe that if $a^- = a^+$, the result reduces to the classical theorem of Oleinik [5]. Furthermore, if $u^- = u^+ = \bar{u}$ for all n, then by the monotonicity condition **(M1)**, we have

$$h(a, \bar{u}) \equiv \bar{h}, \qquad \forall a^- \leq a \leq a^+\,.$$

In this case we trivially have $u_n(t,x) \equiv \bar{u}$, and the theorem holds.

In the rest of the proof, we consider $a^- \neq a^+$ and $u^- \neq u^+$. Without loss of generality, we only consider the case

$$a^- < a^+, \quad u^- < u^+, \quad \text{and} \quad \frac{\partial h}{\partial a} \geq 0\,, \tag{5.4}$$

while all the other cases being similar. The proof take several steps.
Step 1 Similar to the proof of Theorem 2.1 in [4], we consider a decreasing sequence $\delta_n \to 0$, and define the modified flux

$$H_n(x,u) \doteq h(a_n(x),u) + \delta_n(u^+ - u)(u - u^- + a_n(x) - a^-)\,. \tag{5.5}$$

For every $n \geq 1$, we claim that the viscous conservation law

$$u_t + H_n(x,u)_x = \varepsilon_n u_{xx} \tag{5.6}$$

admits a monotone increasing stationary profile U_n with

$$\lim_{x\to-\infty} U_n(x) = u^-, \qquad \lim_{x\to+\infty} U_n(x) = u^+\,. \tag{5.7}$$

Notice that $u(t,x) = U(x)$ is a stationary solution of (5.6) if and only if $U(\cdot)$ satisfies the ODE

$$\varepsilon_n\, U' = \phi_n(x,U) \doteq H_n(x,U) - \bar{h}, \tag{5.8}$$

where

$$\bar{h} = h(a^-,u^-) = h(a^+,u^+).$$

It suffices to show that the ODE (5.8) admits a monotone solution that satisfies (5.7).

Indeed, by the monotonicity condition $\partial h/\partial a \geq 0$, the graph of $u \mapsto h(a^+,u)$ must lie above that of $u \mapsto h(a^-,u)$ on the interval $u \in [u^-,u^+]$. Thus, we have $h(a^+,u) \geq \bar{h}$ on the interval $u \in (u^-,u^+)$. This implies

$$\lim_{x\to+\infty} \phi_n(x,u) > 0, \qquad \text{for } u \in (u^-,u^+)\,.$$

Given x, let $\mathcal{U}_n(x)$ be the largest value of u^0 such that $\phi_n(x,u) > 0$ on the interval $u \in (u^-,u^0)$. Then, $x \mapsto \mathcal{U}_n$ is a monotone function, possibly discontinuous, and

$$\phi_n\left(x,\mathcal{U}_n(x)\right) = 0, \qquad \lim_{x\to-\infty} \mathcal{U}_n(x) \geq u^-\,, \qquad \lim_{x\to+\infty} \mathcal{U}_n(x) = u^+\,.$$

Define the open set Ω_n as

$$\Omega_n \doteq \left\{(x,u)\ :\ x \in \mathbb{R},\ u^- < u < \mathcal{U}_n(x)\right\}\,.$$

We have

$$\phi_n(x,u) > 0, \qquad \forall (x,u) \in \Omega_n\,.$$

Note also that

$$\phi_n(x,u^-) > 0, \qquad \text{for} \quad x \text{ sufficiently large}\,.$$

For some typical examples of $\mathcal{U}_n(x)$ and Ω_n, see Fig. 12.

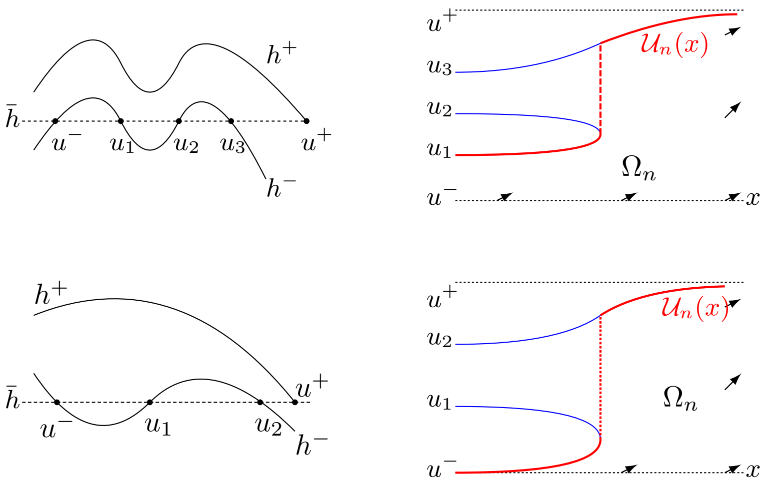

FIGURE 12. Two typical examples. *Left*: plots for $h^-(u)$ and $h^+(u)$. *Right*: On the *blue curves* $\phi_n = 0$, and the thick *red curve* is the discontinuous function $\mathcal{U}_n(x)$. We have $\mathcal{U}_n(-\infty) > u^-$ for the *top* example and $\mathcal{U}_n(-\infty) = u^-$ for the *bottom* one (colour figure online)

Clearly Ω_n is an invariant region for the ODE (5.8), in the sense that if the initial data (x_0, U_0) lies in Ω_n, so will the solution $(x, U(x))$ for all $x \geq x_0$. Furthermore, $U(x)$ is monotone increasing on $x \geq x_0$, and

$$U(x) < \mathcal{U}_n(x) \quad \forall x > x_0, \qquad \lim_{x\to+\infty} U(x) = u^+ . \tag{5.9}$$

Consider now a sequence of solutions with initial data on the lower boundary of Ω_n, i.e., $U(x_0) = u^-$, and set $U_n(x)$ to be the limit solution as $x_0 \to -\infty$. Thus we conclude (5.7), proving the claim.
Step 2 For every $n \geq 1$ and $\tau \geq 0$, by triangle inequality we have

$$\|u_n(\tau,\cdot) - \hat u\|_{\mathbf{L}^1} \;\leq\; \|u_n(\tau,\cdot) - U_n\|_{\mathbf{L}^1} + \|U_n - \hat u\|_{\mathbf{L}^1} . \tag{5.10}$$

It remains to show that, if the constants $\delta_n \downarrow 0$ are suitably chosen, then both terms on the right hand side of (5.10) tend to zero.

Consider the term $\|u_n(\tau,\cdot) - U_n\|_{\mathbf{L}^1}$. Since the evolution equation (5.6) generates a contractive semigroup, regarding u_n as an exact solution and $w(t,x) = U_n(x)$ as an approximate solution, one obtains the error estimate

$$\|u_n(\tau,\cdot) - U_n\|_{\mathbf{L}^1} \leq \|u_n(0,\cdot) - U_n\|_{\mathbf{L}^1} + \int_0^\tau \int \Big| h(a_n, U_n)_x - \varepsilon_n (U_n)_{xx} \Big|\, dx.$$

Using (5.5), the second term on the right-hand side can be bounded by

$$\tau \int \delta_n \Big| \big[(U_n - u^- + a_n - a^-)(u^+ - U_n)\big]_x \Big|\, dx.$$

Putting together, we get the estimate

$$\begin{aligned}\|u_n(\tau,\cdot)-U_n\|_{\mathbf{L}^1} \;\le\; & \|u_n(0,\cdot)-\hat{u}\|_{\mathbf{L}^1}+\|U_n-\hat{u}\|_{\mathbf{L}^1}\\ & + 2\tau\delta_n\left(u^+-u^-\right)\left[(u^+-u^-)+(a^+-a^-)\right].\end{aligned} \tag{5.11}$$

Step 3 By assumption, the initial data satisfy

$$\lim_{n\to\infty}\|u_n(0,\cdot)-\hat{u}\|_{\mathbf{L}^1} \;=\; 0\,.$$

To complete the proof, it suffices to construct a sequence $\delta_n \downarrow 0$ so that, as $n\to\infty$, we have

$$\lim_{n\to\infty}\|U_n-\hat{u}\|_{\mathbf{L}^1} \;=\; 0\,. \tag{5.12}$$

Let $U_n(x)$ be the stationary profile as constructed in Step 1. Then, we have $U_n(0)\ge u^-$ for all n. On the interval $x>0$, let $U_n^\flat$ be the solution of the ODE

$$\varepsilon_n (U_n^\flat)' = \delta_n(u^+-U_n^\flat)(U_n^\flat-u^-+a_n(x)-a^-)\,, \qquad U_n^\flat(\varepsilon_n)=u^-. \tag{5.13}$$

For n sufficiently large, we have

$$a_n(x)-a^- \ge (a^+-a^-)/2 \qquad \forall x\ge\varepsilon_n.$$

Thus, we have $(U_n^\flat)'>0$ for $x\ge\varepsilon_n, U_n^\flat<u^+$, and $(U_n^\flat)'=0$ for $U_n^\flat=u^+$, and the solution satisfies

$$\lim_{x\to+\infty}U_n^\flat(x)=u^+.$$

Furthermore, the difference $\left(u^+-U_n^\flat(x)\right)$ approaches 0 at an exponential rate with the exponent $\mathcal{O}\left(\delta_n/\varepsilon_n\right)$, and thus is integrable on the interval $x>\varepsilon_n$ for every ε_n and δ_n. Therefore, we have, for some constant $\tilde{M}$,

$$\int_{\varepsilon_n}^{+\infty}\left[u^+-U_n^\flat(x)\right]\,dx=\frac{\delta_n}{\varepsilon_n}\tilde{M}. \tag{5.14}$$

For n sufficiently large, we have $U_n(\varepsilon_n)>u^-$. A standard comparison argument gives

$$u^+\ge U_n(x)\ge U_n^\flat(x) \qquad \forall x\ge\varepsilon_n. \tag{5.15}$$

See Fig. 13 for an illustration. Thus, by (5.14) we have, for some constant M,

$$\int_{\varepsilon_n}^{+\infty}\left[u^+-U_n(x)\right]\,dx=\frac{\delta_n}{\varepsilon_n}M. \tag{5.16}$$

For $x<0$, we discuss two cases. First, consider the bottom case in Fig. 12. Since h is a smooth function, then as a_n converges to the jump function (1.7) in $\mathbf{L}^1$, the function $\mathcal{U}_n$ converges to $\hat{u}$ in $\mathbf{L}^1$. Thanks to the bounds

$$u^-\le U_n(x)\le\mathcal{U}_n(x), \qquad \forall x,$$

a squeezing argument implies that

$$\lim_{n\to+\infty}\int_{-\infty}^{0}(U_n(x)-u^-)\,dx=0\,. \tag{5.17}$$

Finally, consider the top case in Fig. 12, and write

$$w^- \;\doteq\; \lim_{n\to+\infty}\mathcal{U}_n(x)>u^-.$$

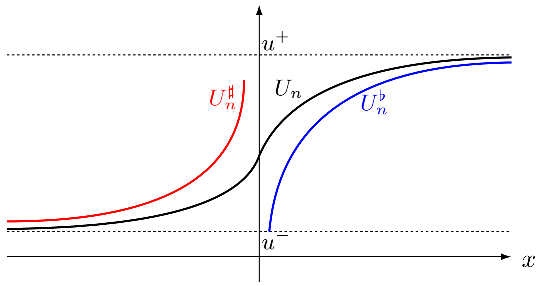

FIGURE 13. Illustration of $U_n, U_n^\flat$ and $U_n^\sharp$

In this case, we have

$$\lim_{n\to\infty} \mathcal{U}_n(x) = \begin{cases} u^+, & (x>0), \\ w^-, & (x>0). \end{cases}$$

For $x < -\varepsilon_n$, let $U_n^\sharp$ be the solution of the following ODE

$$\varepsilon_n (U_n^\sharp)' = \delta_n (u^+ - U_n^\sharp)(U_n^\sharp - u^-), \qquad U_n^\sharp(-\varepsilon_n) = w^-. \tag{5.18}$$

Again, as $x \to -\infty$, the function $U_n^\sharp$ approaches u^- at an exponential rate with the exponent $\mathcal{O}\left(\frac{\delta_n}{\varepsilon_n}\right)$. Thus, we have the following estimate,

$$\int_{-\infty}^{-\varepsilon_n} \left[U_n^\sharp(x) - u^-\right] dx = \frac{\delta_n}{\varepsilon_n} M, \qquad \text{for some constant } M. \tag{5.19}$$

For n sufficiently large, we have $U_n(-\varepsilon_n) \le w^-$. Again, a comparison argument gives

$$u^- \le U_n(x) \le U_n^\sharp(x), \qquad \forall x < -\varepsilon_n\,. \tag{5.20}$$

Combining (5.16), (5.15), (5.17), (5.19) and (5.20), we finally arrive at

$$\begin{aligned} \|U_n - \hat{u}\|_{\mathbf{L}^1} &\le \int_{-\infty}^{-\varepsilon_n} \left(U_n^\sharp(x) - u^-\right) dx + 2\varepsilon_n \left(u^+ - u^-\right) \\ &\quad + \int_{\varepsilon_n}^{\infty} \left(u^+ - U_n^\flat(x)\right) dx \\ &= 2M\frac{\delta_n}{\varepsilon_n} + 2\varepsilon_n \left(u^+ - u^-\right). \end{aligned}$$

The limit (5.12) is achieved by assuming $\delta_n/\varepsilon_n \to 0$ and $\varepsilon_n \to 0$ as $n \to \infty$, completing the proof. $\square$

5.2. Triangular systems

We remark that a similar result of Theorem 5.1 holds for the triangular system (1.11) and its approximation (4.14), obtained by a similar proof as for Theorem 5.1. The viscous shock α_n for the second equation in (4.14) is monotone, therefore we only need the monotonicity of the mapping $\alpha \mapsto h$. We state the Theorem below, and omit the proof.

Theorem 5.2. *Consider the triangular system (1.11) and the viscous approximation (4.14), with the Riemann data $(u^\pm, \alpha^\pm)$. Assume that*

$$\alpha^- < \alpha^+, \quad g(\alpha^-) = g(\alpha^+) = 0, \qquad g(\alpha) > 0 \quad \text{for} \quad \alpha^- < \alpha < \alpha^+.$$

Let $\varepsilon_n, \varepsilon_n'$ be two convergent sequences such that

$$\lim_{n\to\infty} \varepsilon_n = 0, \qquad \lim_{n\to\infty} \varepsilon_n' = 0.$$

Let u^-, u^+ be two states which satisfy the admissible conditions in Theorem 2.1, and recall the jump function $\hat{u}$ in (2.5). Let $u_n = u_n(t,x)$ be a sequence of solutions to the viscous system (4.14), where the initial data $u_n(0,x)$ satisfies (5.2). If the following monotonicity condition holds

(M1) *For every u, the function $\alpha \mapsto h(\alpha, u)$ is monotone. Namely, either $\dfrac{\partial h}{\partial \alpha}(\alpha, u) \geq 0$ or $\dfrac{\partial h}{\partial \alpha}(\alpha, u) \leq 0$ for all α, u.*

Then, we have the convergence (5.3), uniformly as τ ranges in bounded sets.

5.3. Polymer flooding models

The application of Theorems 5.1 and 5.2 to the polymer flooding models (1.6) in Lagrangian coordinate is straight forward. It is useful to translate the monotonicity condition (**M1**) into a condition relating to the flux function $f(s,c)$ for the Eulerian models (1.3) and (1.1).

We claim that, this monotone assumption is equivalent to the monotone assumption on the flux function $c \mapsto f(s,c)$. This means, if $c \mapsto f(s,c)$ is monotone, then the graphs of the mappings $(1/f(s,c_1)) \mapsto (-s/f(s,c_1))$ and $(1/f(s,c_2)) \mapsto (-s/f(s,c_2))$ for two distinct values of c_1, c_2 never crosses each other. Indeed, if the graphs intersect at a point, then we must have, for some s_1, s_2

$$\frac{1}{f(s_1,c_1)} = \frac{1}{f(s_2,c_2)}, \qquad \frac{s_1}{f(s_1,c_1)} = \frac{s_2}{f(s_2,c_2)}.$$

This implies $s_1 = s_2 = s$, which further implies $f(s,c_1) = f(s,c_2)$ for this s, a contradiction to the monotone assumption on $c \mapsto f(s,c)$.

Thus, under the monotone assumption

$$\frac{\partial f(s,c)}{\partial c} < 0, \qquad \forall (s,c), \tag{5.21}$$

Theorem 5.2 ensures that all vanishing viscosity limits for the system (1.6) in Lagrangian coordinate are the same. We remark that, the monotone assumption (5.21) has a physical interpretation: the water phase has lower mobility if it is dissolved with more polymers.

We remark that, for the viscous approximation (4.19) in Eulerian coordinates, the convergence result for vanishing viscosity is still open. We are tempted to conjecture that all vanishing viscosity limits $\varepsilon_1, \varepsilon_2 \to 0$ are the same if (5.21) holds.

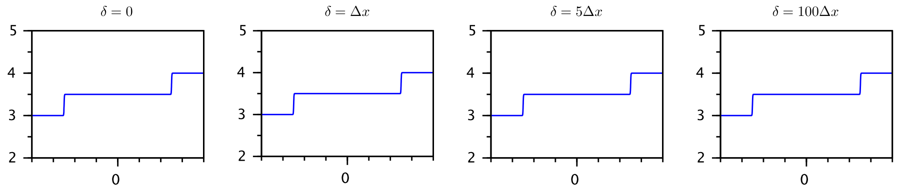

FIGURE 14. Simulation results for Example 6.1

6. Concluding remarks

We remark that the monotonicity conditions (**M1**)–(**M2**) are sufficient, but not necessary. We offer a simple example.

Example 6.1. *We revise Example 4.4, and let*

$$h(a, u) = -(1 - a)(u - 2)^2 - a(u - 5)^2.$$

*We see that $h^L(u), h^R(u)$ are the same as in Example 4.4. Note also that the graphs of h^L, h^R cross each other at $u = 3.5$, where the partial derivative $\frac{\partial h}{\partial a}$ changes sign, so the monotonicity condition (**M1**) fails. However, the numerical simulations, plotted in Fig. 14, indicate unique vanishing viscosity limit. The admissible a-jump occurs at the intersection point of the graphs of h^L, h^R, which is the same limit as in Theorem 2.1. Simple sketches of the vector fields for the ODE (4.18) satisfies by the traveling waves would lead to the same conclusion.*

One may conjecture that some weaker assumptions suffice. However, a precise formulation of a necessary condition and a detailed proof of uniqueness with such assumptions seem challenging.

Acknowledgements

The author acknowledges useful discussion with Graziano Guerra, from University of Milano-Bicocca in Italy, which led to the construction of Example 4.4.

References

[1] Andreianov, B.: New approaches to describing admissibility of solutions of scalar conservation laws with discontinuous flux. ESAIM Proc. Surv. **50**, 40–65 (2015)

[2] Buckley, S.E., Leverett, M.: Mechanism of fluid displacement in sands. Trans. AIME **146**, 107–116 (1942)

[3] Gimse, T., Risebro, N.H.: Riemann problems with a discontinuous flux function. In: Engquist, B., Gustafsson, B. (eds). Proceedings of Third International Conference on Hyperbolic Problems. Theory, Numerical Method and Applications. Studentlitteratur/Chartwell-Bratt, Lund-Bromley, pp. 488–502 (1991)

[4] Guerra, G., Shen, W.: Vanishing viscosity solutions of Riemann problems for models of polymer flooding. In: Gesztesy, F., Hanche-Olsen, H., Jakobsen, E., Lyubarskii, Y., Risebro, N., Seip, K. (eds). To appear in "Partial Differential Equations, Mathematical Physics, and Stochastic Analysis". A Volume in Honor of Helge Holden's 60th Birthday. EMS Congress Reports. (2017)

[5] Oleinik, O.: Uniqueness and stability of the generalized solution of the Cauchy problem for a quasilinear equation. Uspehi Mat. Nauk. **14**(2) (86), pp. 165-170 (1959) (Russian). English Translation in Amer. Math. Soc. Transl. Ser. 2, **33**, pp. 285–290 (1964)

[6] Pires, A.P., Bedrikovetsky, P.G., Shapiro, A.A.: A splitting technique for analytical modelling of two-phase multicomponent flow in porous media. J. Pet. Sci. Eng. **51**, 54–67 (2006)

[7] Shen, W.: On the Cauchy problems for polymer flooding with gravitation. J. Differ. Equ. **261**, 627–653 (2016)

[8] Shen, W.: Scilab codes for all the simulations presented in this paper can be found at: http://www.personal.psu.edu/wxs27/SIM/BressanSISSA

[9] Temple B.: Stability and decay in systems of conservation laws. In: Carasso, C., Raviart, P.A., Serre, D. (eds). Proceeding of Nonlinear Hyperbolic Problems. Springer-Verlag, New York, (1986)

[10] Tveito, A., Winther, R.: Existence, uniqueness, and continuous dependence for a system of hyperbolic conservation laws modeling polymer flooding. SIAM J. Math. Anal. **22**(4), 905–933 (1991)

[11] Wagner, D.: Equivalence of the Euler and Lagrangian equations of gas dynamics for weak solutions. J. Differ. Equ. **68**, 118–136 (1987)

Wen Shen
Mathematics Department
Pennsylvania State University
University Park
PA 16802
USA
e-mail: wxs27@psu.edu

Received: 28 December 2016.
Accepted: 31 May 2017.